ISSN 1070-4272, Russian Journal of Applied Chemistry, 2009, Vol. 82, No. 8, pp. 1357−1363. © Pleiades Publishing, Ltd., 2009.
Original Russian Text © Yu. Mirgorod, N.A. Borshch, A.A. Reutov, G.Yu. Yurkov, V.M. Fedosyuk, 2009, published in Zhurnal Prikladnoi Khimii, 2009, Vol. 82, No. 8, pp. 1261−1267.

INORGANIC SYNTHESIS AND INDUSTRIAL INORGANIC CHEMISTRY

Synthesis of Gadolinium-Based Nanoparticles in a System of Direct Surfactant Micelles and Study of Their Magnetic Properties

Yu. Mirgorod[a], N. A. Borshch[b], A. A. Reutov[a], G. Yu. Yurkov[c], and V. M. Fedosyuk[d]

[a] *Kursk State University, Kursk, Russia*
[b] *Kursk State Technical University, Kursk, Russia*
[c] *Baikov Institute of Metallurgy and Materials Science, Russian Academy of Sciences, Moscow, Russia*
[d] *Scientific-Practical Center of the National Academy of Belarus for Materials Science, State Research-and-Production Association, Institute of Solid-State and Semiconductor Physics, National Academy of Belarus, Minsk, Belarus*

Received February 18, 2009

Abstract—Synthesis method is suggested and the size and shape of Pt–Gd particles formed in reduction of metal ions in an aqueous system of direct micelles were determined in relation to the concentration of surfactants and reducing agents: hydrazine hydrate, quercetin, and rutin. The magnetic properties of the nanoparticles obtained were studied.

DOI: 10.1134/S1070427209080072

At present, nanomaterials and nanotechnologies are at the focus of researchers' and designers' attention [1–3]. A particular place in this area is occupied by magnetic nanomaterials and nanostructures [1, 4–6], which can be used in various magnetic microelectronic devices: high-efficiency shields; information recording, storage, and reading devices; various transducers, etc. [7]. They can also be applied in medicine and biotechnologies.

Metal nanoparticles are commonly synthesized in inverse micelles [8]. To obtain nanoparticles in direct micelles, it is first necessary to synthesize functional surfactants, e.g., $Gd(DS)_3$, where DS is the dodecyl sulfate ion, and then to obtain Gd nanoparticles in direct micelles, using more readily available DSNa surfactants. It is commonly believed that the electric double layer of a micelle acts as a template in this case.

It has been shown previously [9] that Pt–Ni nanoparticles can be produced in direct micelles of ordinary surfactants. In this case, the inorganic and organic ions of a surfactant may be of the same sign, e.g., Gd^{3+} and $C_{16}H_{33}C_5H_5N^+$. The mechanism of such a synthesis cannot be explained in terms of the classical model of a direct micelle, i.e., a hydrocarbon drop coated with an electric double layer.

To explain the synthesis mechanism, it is necessary to apply a dualistic model of the micelle, which is a superposition of a contact and hydrated micelles [10]. A hydrated micelle, into which inorganic ions penetrate and are afterwards reduced by various reducing agents, can serve as a template.

The aim of our study was to demonstrate the possibility of synthesis of magnetic bimetallic Pt–Gd particles in direct micelles, examine the effect of the nature and concentration of a surfactant, reducing agents, and platinum on the synthesis of nanoparticles, and analyze their magnetic properties.

EXPERIMENTAL

We used the following main reagents: cetylpyridinium chloride $C_{16}H_{33}C_5H_5NCl$ (CPC) and sodium bis(2-ethylhexyl) sulfosuccinate $C_{20}H_{37}NaO_7S$ (AOT), which differ in structure from the previously used cetyltrimethylammonium chloride [9]; gadolinium acetate $Gd(CH_3COO)_3$; platinohydrochloric acid $H_2[PtCl_6]$; hydrazine hydrate $N_2H_4 \cdot H_2O$; quercetin (3,3',4',5,7-pentahydroxyflavone); and rutin (quercetin 3-0-ramnoglucoside) manufactured by Sigma-Aldrich.

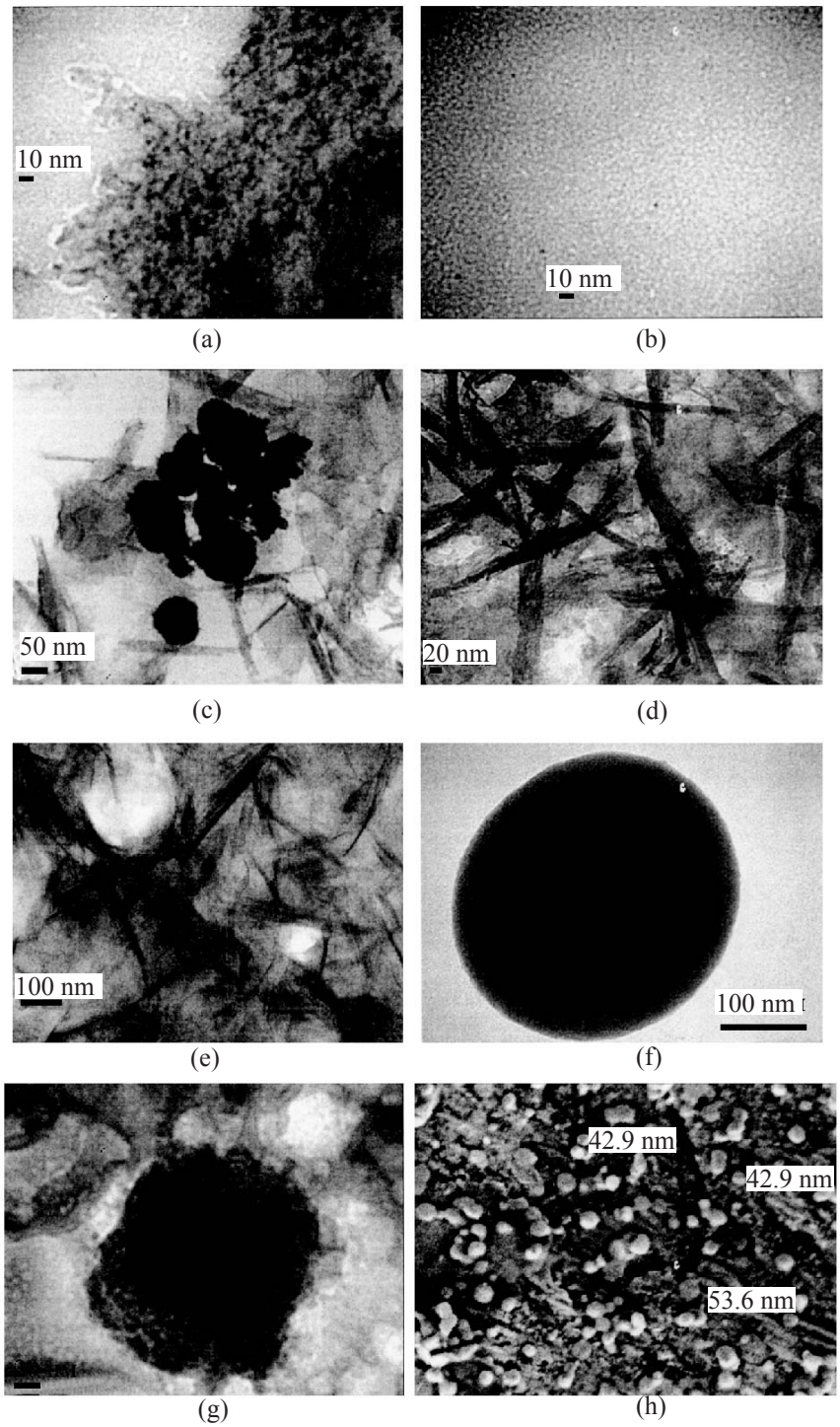

Fig. 1. Micrographs of the reaction mixture. (a, b) CPC concentration 2.93×10^{-2} M, (c) CPC concentration 2.93×10^{-3} M, (d) no $H_2[PtCl_6]$, (e) CPC concentration (5×10^{-4} M) lower than the CMC, (f) reduction with quercetin, (g) reduction with rutin, and (h) SEM micrograph of the reaction mixture in synthesis with AOT.

The purity of CPC and AOT was additionally checked by the absence of a minimum near the critical micelle concentration (CMC) on the surface tension isotherm of aqueous solutions of CPC and AOT, measured by the method of detachment of a platinum plate. The CMCs for CPC and AOT, found from the bend in this function,

are 6.2×10^{-4} and 2.18×10^{-3} M. The rest of the reagents were used without additional purification.

We performed the synthesis in a test tube of a UZDN low-frequency ultrasonic disperser with a working frequency of 44 kHz. The electrical oscillations in the disperser were produced by a 400-W generator. These oscillations were converted by magnetostriction transducers to elastic mechanical vibrations, which acted via a tubular radiator (in which the test tube for nanoparticle synthesis was placed) on the medium being dispersed. The tubular radiator was cooled with flowing water. The synthesis temperature was maintained at 25 ± 1°C. The size and shape of nanoparticles were determined with a JEOL JEM-1011 transmission electron microscope at an accelerating voltage of 100 kV. Prior to being studied, the suspension obtained in the experiment was agitated with a UZDN-2 ultrasonic disperser (oscillation frequency 22 kHz, exposure duration 10 min). It was verified that the size of nanoparticles remained unchanged during the agitation. A drop of the suspension was deposited onto a copper grid successively coated with layers of polyvinyl formal and carbon, transparent to electrons.

The content of platinum in the Pt–Gd powder was determined on a Kvant-Z atomic-absorption spectrometer with an electrothermal atomizer (graphite furnace) at a wavelength of 265.9 nm, with a detection limit of 3 μg l^{-1}. The solutions used were prepared by the method described in [11].

The magnetic studies were carried out on a "magnetic balance" by the ponderomotive method [12] and on versatile Cryogenic high-field measurement system [13]. In addition to ordinary measurements of the magnetic moment as a function of the magnetic field and temperature, we also measured the magnetic susceptibility upon zero field cooling (ZFC) and low field cooling (FC) in magnetic fields [5, 14]. This method is commonly used to examine the so-called granulated systems (or nanostructured alloys) [3, 4, 14], when the system exhibits a superparamagnetic behavior. The characteristic maximum on the ZFC curve at the blocking temperature [3–5] can be used to estimate the size of nanoparticles and the size distribution of nanoparticles or nanoinclusions.

(1) Synthesis of Pt–Gd nanoparticles with a CPC concentration exceeding the CMC. A 0.2585-g portion of CPC was placed in a test tube (2.93×10^{-2} M in the whole volume) and bubbled with nitrogen for 3 min to remove atmospheric oxygen, and then 21 ml of distilled water, 0.14 ml of 0.14 M $H_2[PtCl_6]$ (7.5×10^{-4} M in the whole volume), and 3 ml of a 0.14 M aqueous solution of $Gd(CH_3COO)_3$ (1.6×10^{-2} M in the whole volume) were added. Nitrogen was passed through the solution for 4 min and then it was agitated for 10 min to give a yellowish solution. It was found that the yellow color of the solution is due to the interaction of $[PtCl_6]^{2-}$ with $C_{16}H_{33}C_5H_5N^+$. Then redox reactions of $[PtCl_6]^{2-}$ and Gd^{3+} with hydrazine hydrate were commenced in an alkaline medium

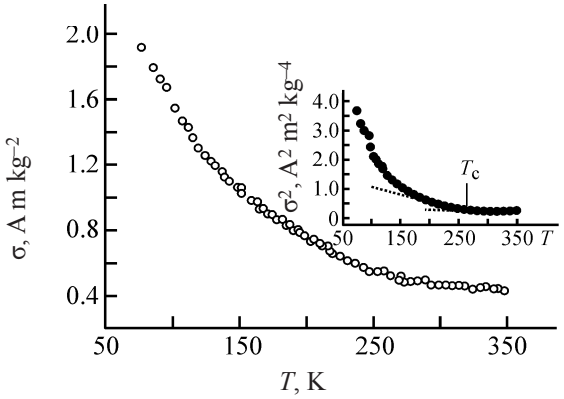

Fig. 2. Specific magnetization σ and squared specific magnetization (inset) of the Gd–Pt nanopowder vs. temperature *T*. Sample mass $m = 0.0093$ g, $H = 0.86$ *T*.

$$2H^+ + [PtCl_6]^{2-} + N_2H_4 + 6OH^- = Pt + 6Cl^- + N_2 + 6H_2O,$$

$$Gd^{3+} + N_2H_4 + 4OH^- = Gd + N_2 + 4H_2O.$$

For this purpose, 3 ml of a 0.6 M solution of N_2H_4 (6.9×10^{-2} M in the whole volume) was added and the mixture was agitated for 10 min. In the process, the color of the solution remained unchanged. Further, 2 ml of a 2 M solution of KOH was introduced (0.15 M in the whole volume) and the mixture was agitated for additional 10 min. The solution started to darken because of the formation of nanoparticles, whose coarsening yielded a beige-brown dispersion. After the experiment was complete, a dark brown precipitate appeared on the bottom of the test tube. To isolate the metallic powder obtained, the solution was centrifuged (at 5000 rpm), decanted, washed with ethanol to remove the CPC, and again centrifuged and decanted. This yielded a dark brown bimetallic (Pt–Gd) powder for a study with a magnetometer. The resulting nanosize material contained 2.4 wt % Pt which in fact corresponded to full reduction of platinum from platinohydrochloric acid.

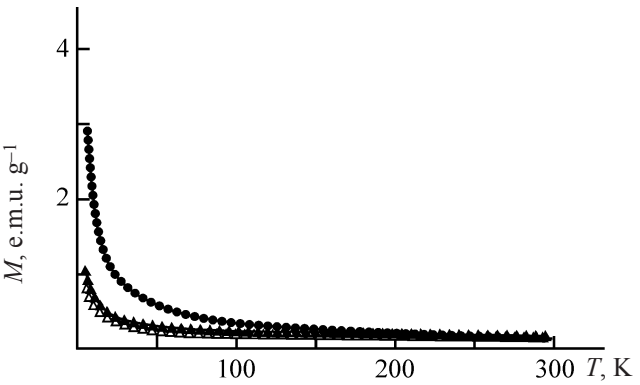

Fig. 3. ZFC–FC curves. (*M*) Magnetic moment and (*T*) temperature; the same for Fig. 4. Cooling and heating in fields of 0.05 and 0.2 *T*.

The experimentally obtained dispersion was studied by transmission electron microscopy (TEM). As can be seen in Fig. 1a, the Pt–Gd nanoparticles formed are distributed as conglomerates in a special structure of the dispersion, formed by CPC and nanoparticles with the rest of the dispersion. The size of the nanoparticles synthesized can be determined from Figs. 1a and 1b to be 5 to 10 nm. As the CPC concentration was lowered to 2.93×10^{-3} M, the light-colored solution darkened and then a black finely dispersed precipitate was formed. It was demonstrated by means of TEM that coarser Pt–Gd nanoparticles about 50 nm in size are formed in these conditions and, in turn, gather into conglomerates 150 to 300 nm in size on the background of CPC crystals or mesophases (Fig. 1c).

(2) Synthesis without H_2[PtCl]. As demonstrated in [6], bimetallic platinum-containing nanoparticles are synthesized with platinum catalyzing this process. It is known that the above method of synthesis cannot be used for obtaining homometallic particles, e.g., those of Ni [3]. In the present study, we tested this method as applied to synthesis of Gd nanoparticles. For this purpose, we carried out an experiment in which 0.14 ml of water was introduced into the test tube, instead of a $H_2[PtCl_6]$ solution, with the rest of the procedure being the same as that in the first run. A light-colored solution was obtained in which no reactions were visually detected. Figure 1d demonstrates the formation of rod-like CPC crystals (or mesophases). No Pt–Gd particles could be observed in all the six micrographs obtained in this case.

(3) Synthesis of Pt–Gd nanoparticles at a CPC concentration lower than the CMC. The synthesis conditions were the same as those in the first run. The CPC concentration was lowered to 5×10^{-4} M. Visually, the same pattern as that in run no. 2 was observed.

(4) Synthesis of Pt–Gd particles with reduction by quercetin. In the patent [15], it is suggested to use natural compounds from the flavonoid group, quercetin and rutin, as agents for reducing metal ions in the system of inverse surfactant micelles. Use of flavonoids as reducing agents makes it possible to raise the reduction rate and to obtain stable metal nanoparticles in the presence of atmospheric oxygen. In the given experiment, quercetin was used as a reducing agent instead of hydrazine hydrate.

A test tube was charged with 0.26 g of CPC and 0.14 ml of a 0.14 M solution of $H_2[PtCl_6]$, the mixture was bubbled with nitrogen for 3 min, and then 23 ml of water, 3 ml of a 0.14 M solution of $Gd(CH_3COO)_3$, and 4 mg of quercetin were added. The solution was bubbled with nitrogen for 4 min and dispersed in an ultrasonic field for 30 min. As a result, a light-colored solution with white flakes was obtained. As can be seen in Fig. 1f, the reduction of Pt and Gd ions by quercetin yields coarse Pt–Gd particles 100–500 nm in size, coated with a sheath composed of CPC and quercetin.

(5) Synthesis of Pt–Gd nanoparticles with reduction by rutin. Nanoparticles were synthesized by the procedure described in run no. 4, with the only difference that 10 mg of rutin was used instead of quercetin. During the synthesis, a pattern similar to that in the first run was visually observed. Upon addition of rutin and beginning of an ultrasound dispersion, the solution started to darken, then fine particles were formed and coarsened to form a dark dispersion. An analysis for the content of platinum yielded a value of 2.3 wt %, which approximately corresponds to full reduction of $[PtCl_6]^{2-}$, as in the first run. It follows from Fig. 1g that the Pt–Gd particles formed in this case are finer (5–10 nm) than those obtained in reduction with quercetin.

(6) Synthesis of Pt–Gd nanoparticles at an AOT concentration exceeding the CMC. A 0.2323-g portion of AOT (2.2×10^{-2} M in the whole volume) was bubbled with nitrogen for 3 min. Then 14.41 ml of distilled water, 2.06 ml of a 0.13 M aqueous solution of $Gd(CH_3COO)_3$, 0.096 ml of a 0.14 M aqueous solution of $H_2[PtCl_6]$, and 2.06 ml of a 0.6 M aqueous solution of N_2H_4 were added. The mixture was bubbled with nitrogen for 3 min and agitated with the ultrasonic disperser for 15 min. Further, 1.37 ml of a 2 M KOH solution was added and the mixture was agitated for additional 15 min. After the alkali was introduced into the reaction mixture, the solution started

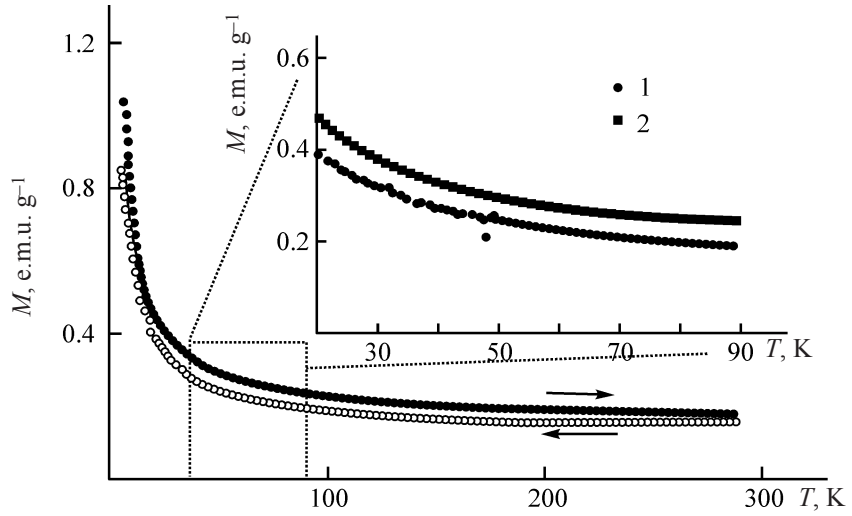

Fig. 4. ZFC–FC curve measured in a field of 500 Oe by the standard method (cooling in zero field, heating in a field of 500 Oe to 290 K, and cooling in this field to 6 K).

to darken. Black particles gradually precipitated from the solution and formed a black suspension. In a micrograph of the dispersion, obtained using a scanning electron microscope, metallic nanoparticles 40 to 50 nm in size can be seen on the background of AOT (Fig. 1h).

As can be seen in Fig. 1, three cases are observed when the dispersion is obtained: (1) CPC crystals (mesophases) are formed (Figs. 1d, 1e); (2) coarse Pt–Gd particles are produced (Figs. 1c, 1f); and Pt–Gd nanoparticles are formed together with a particular structure seen in the micrographs (Figs. 1a, 1b, 1g, 1h). These observations agree with the commonly accepted concepts of phase separation.

It follows from the experimentally confirmed theoretical concepts that the transition of a system (solution) from the single-phase state to a two-phase state can occur by different mechanisms [16].

First, a crystalline phase can be formed on the binodal from a metastable state between the binodal and spinodal.

The second mechanism of phase separation becomes operative as the system reaches the spinodal [17]. The spinodal decomposition, i.e., a phase transition involving unstable states, has no directed flows of mass and(or) energy and, e.g., in the case of binary liquid systems, is characterized by very short duration. However, the existence time of the spinodal structure increases in the presence of a surfactant [18]. In this case, if formed under irreversibility and dissipation conditions, the new structure is stabilized by the existence of directed flows of mass and(or) energy, e.g., the dispersion energy.

This general approach does not contradict the concept of dual properties of surfactant micelles, which are, simultaneously, heterogeneous and homogeneous concentration fluctuations exhibiting a good dissolving capacity for the accompanying substances [19] from which nuclei of new phases can be formed. In the spinodal decomposition, two phases kind of penetrate into each other (Figs. 1a, 1b, 1g, 1h). Naturally, they form different microphases in the absence of water. Therefore, Figs. 1a, 1b, 1g, and 1h show Pt–Gd particles on the background of a "ripple" of the spinodal decomposition.

According to reference data, the specific magnetization σ of bulk Gd single crystals in fields of 0.5–1.7 T in the atmosphere of nitrogen is 240 A m_3 kg^{-2} and has a Curie point of about 293 K. The specific magnetization of a Pt–Gd powder obtained in the first synthesis in amicellar solution of CPC was measured on a magnetic balance in a field of 0.86 T. It was found that its specific magnetization is two orders of magnitude lower than that of Gd single crystals and has a value of 1.92 A m^3 kg^{-2}. The Curie point of the Pt–Gd nanopowder under study is $T_c \approx 270$ K (Fig. 2), which is approximately 23 K lower than the Curie point of the bulk sample. Figure 3 shows ZFC–FC curves obtained in cooling at different comparatively weak magnetic fields, 0.05 and 0.2 T in the given case. The procedure used to measure this curves consists in the following.

A sample is first cooled in a zero magnetic field. If the sample was in the superparamagnetic state at room

temperature or at higher temperatures, such a cooling results in that chaotically disoriented particles are frozen and, at low temperatures, the magnetic moment must be close to zero, as also it should be at high temperatures, i.e., temperatures above the Curie point T_c for a ferromagnetic or blocking temperature T_b for a superparamagnetic. Then a weak magnetic field is applied and the sample is heated in this field. If nanoparticles are in the superparamagnetic state, then the heating results in that their magnetic moments, tending to be oriented in parallel, must start to interact with one another, and, as a consequence, a maximum at a low temperature named the blocking temperature T_b must appear in the ZFC curve [6, 20]. Upon further heating of the sample, its magnetic moment must first decrease because of the weakening of the interaction between particles, caused by their Brownian motion. Further, in cooling in a weak magnetic field, the magnetic moment of the sample will permanently increase. As can be seen in Figs. 3 and 4, another pattern is observed. The data in Figs. 3 and 4 for a field of 0.05 T differ only in the order of cooling and heating. Figure 4 shows FC–ZFC curves, and Fig. 3, the classical ZFC–FC curves. Naturally, no hysteresis loop would be expected to occur at room temperature, which is undoubtedly higher than the Curie point. At low temperatures, an ordinary hysteresis loop is observed, with leveling-off at sufficiently strong fields (Fig. 4, inset). A certain asymmetry of the hysteresis loop is probably due to the influence of residual fields in the course of measurements (Fig. 4, inset).

Thus, taking into account the results obtained in a study of magnetic properties (Figs. 2–5), we can assume that, in all probability, we obtained Gd nanoparticles with some Pt inclusions and these nanoparticles are enveloped in a sheath having the form of a partially oxidized outer layer and containing residual amounts of chemical reaction products that appeared in synthesis of nanoparticles. It is this "coat" that leads to weakening of the interaction between nanoparticles and, as a consequence, to an "untypical" superparamagnetic behavior: lack of a maximum in ZFC curves.

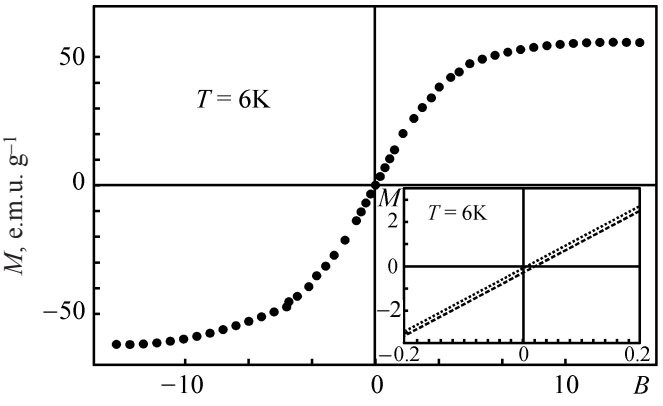

Fig. 5. Remagnetization curve (hysteresis loop) of the Gd–Pt powder under study at 6 K. (*M*) Magnetic moment and (*B*) magnetic susceptibility.

CONCLUSIONS

(1) Conditions were found in which Pt–Gd nanoparticles 5–10 nm in size are synthesized in micellar solutions of cetylpyridinium chloride in the presence of reducing agents, hydrazine hydrate and rutin.

(2) The influence exerted by the nature and concentration of surfactants, reducing agents, and platinum on the synthesis of nanoparticles was studied.

(3) It was shown that the specific magnetization of the nanoparticles synthesized is by two orders of magnitude lower, and the Curie point, by 23 K lower than the respective parameters of the single-crystal sample.

ACKNOWLEDGMENTS

The study was supported in part by the Ministry of Education and Science of the Russian Federation (project no. 1.1.07).

REFERENCES

1. Fedosyuk, F.M., Anishchik, V.M., and Borisenko, V.E., *Nanomaterialy i nanotekhnologii* (Nanomaterials and Nanotechnologies), Minsk: Izd. Tsentr Bel. Gos. Univ., 2008.
2. Fedosyuk, F.M., Labunov, V.A., and Yanushkevich, K.I., *Ros. Nanotekhnol.,* 2008, vol. 3, nos. 3–4, pp. 115–121.
3. Buchachenko, A.L., *Usp. Khim*., 2003, vol. 72, pp. 419–437.
4. Fedosyuk, V.M., *Springer Sci. Business Media*, 2006, pp. 1750–1757.
5. Fedosyuk, V.M., *Handbook of Powders of Non-Ferrous Metals*, Elsevier Advanced Technology, 2007.
6. Gubin, S.P., Koksharov, Yu.A., Khomutov, G.B., and Yurkov, G.Yu., *Usp. Khim*., 2005, vol. 74, no. 6, pp. 539–574.
7. Yurkov, G.Yu., Fionov, A.S., Koksharov, Yu.A., et al., *Neorg. Mater*., 2007, vol. 43, no. 8, pp. 936–947.

8. Pileni, M.P., *Langmuir*, 1994, vol. 13, pp. 3266–3276.
9. Mirgorod, Yu.A. and Efimova, N.A., *Zh. Fiz. Khim.,* 2008, no. 3, pp. 465–469.
10. Mirgorod, Yu.A., *Zh. Strukt. Khim*., 2008, vol. 49, no. 3, pp. 920–925.
11. RF Patent 2226224.
12. Chechernikov, V.I., *Magnitnye izmereniya* (Magnetic Measurements), Moscow: Mosk. Gos. Univ., 1969.
13. www.cryogenic.co.uk
14. Yurkov, G.Yu., Gubin, S.P., Pankratov, D.A., et al., *Neorg. Mater*., 2002, vol. 38, no. 2, pp. 186–195.
15. RF Patent 2147487.
16. Prigogine, I., *Chemical Thermodynamics*, Longmans, Green, 1954.
17. Skripov, V.P. and Skripov, A.V., *Usp. Fiz. Nauk*, 1979, vol. 123, no. 2, pp. 193–231.
18. Roux, D., *J. Physique*, 1986, vol. 47, pp. 733–738.
19. Yurkin, V.G., *Usp. Khim*., 1995, vol. 64, no. 3, pp. 237–250.
20. Fedosyuk, F.M., *Nanostrukturnye plenki i nanoprovoloki* (Nanostructured Films and Nanowires), Minsk: Izd. Tsentr Bel. Gos. Univ., 2006.